Bulletin of the Seismological Society of America, Vol. 102, No. 5, pp. 2225–2231, October 2012, doi: 10.1785/0120120092

Ⓔ

Short Note

Local Site Response in an Alpine Valley from Recorded Earthquakes and Ambient Noise Analysis

by Carla Barnaba and Alessandro Vuan

Abstract Local response is estimated within the sediment fill of the Tagliamento River Valley (THV), northeastern Italy, using about 90 weak-to-medium local and regional earthquakes. Ground motion is recorded at six stations deployed in a linear array across the valley. Site amplification factors are determined using the standard spectral ratio, the generalized inversion technique, and evaluations of receiver functions. Results obtained from earthquake data are then compared with ambient noise analysis. Azimuthal effects in the seismic response are observed locally for waves coming from the east-southeast, aligned with the longitudinal axis of the valley. The seismic responses evaluated at the mid-valley and at the valley edge are then convolved with the 1976 M_w 6.4 Friuli mainshock recorded at accelerometric station TLM1, located close to the array. The local response at the valley edge, in the town of Cavazzo Carnico, is responsible for an enhancement of the input motion of an average factor of about 4 in the frequency range from 2 to 8 Hz. The elastic demand from the current national regulation for a 475-year return period and specific for Cavazzo Carnico is overcome by the 5%-damped pseudoacceleration response spectrum estimated at the valley edge. The underestimation of the Italian code is mostly due to a 2D amplification effect at the valley edge rather than a simple inadequacy of the V_{S30} site classification.

Online Material: Figures showing locations of historical earthquakes, distribution of fundamental frequency of vibration, waveforms of the M_D 5.1 Kobarid earthquake, *S*-wave velocity versus depth, and GIT and RF amplification median values and spectra; tables of seismic station locations and soil type, and of local and regional earthquakes.

Introduction

The high valley of the Tagliamento River (THV), between the towns of Tolmezzo and Cavazzo Carnico (northeastern Italy; see Fig. 1) has been hit in the past by several earthquakes, the best documented of which are the events of 1928 and 1976 (Ⓔ see Fig. S1 available in the electronic supplement to this paper). The Italian macroseismic database (DBMI04, see Data and Resources; Stucchi *et al.*, 2007) indicates higher damage in Cavazzo Carnico (I_0 = IX, MCS) than in Tolmezzo (I_0 = VIII). The geological and geomorphologic maps in Cavazzo and Tolmezzo do not fully explain the different site responses over a distance of a few kilometers (Brisighella *et al.*, 1976). However, it is well known that local conditions can strongly influence ground motions during earthquakes (e.g., Bard and Bouchon, 1985; Pedersen *et al.*, 1995; Field, 1996; Kawase, 1996). In particular, because of the sediment fill and subsurface topography, the Alpine valleys can generate 2D and 3D amplification effects. This behavior is strictly linked to the width and depth of the THV and to the direction of the incident wave field. In shallow valleys, when the depth is small in comparison with the width, the wave field is dominated by laterally propagating surface waves generated at the valley edges (Field 1996; Chávez-García *et al.*, 2002). A 1D resonance is the prevailing effect due to interference between bedrock and sediments (e.g., Fäh *et al.*, 1993).

In deeper valleys the interference of surface waves with vertical propagating waves gives rise to the evolution of a 2D resonance pattern. This phenomenon is well described by numerical simulations (e.g., Bard and Bouchon, 1985; Steimen *et al.*, 2003; Frischknecht and Wagner, 2004), but few observations are available on real data (Kagami *et al.*, 1982; Tucker and King, 1984; Roten *et al.*, 2006). To better understand and quantify the seismic response of the Alpine valleys, a European Union INTERREG Sismovalp (Seismic Hazard and Alpine Valley Response Analysis) Project was carried out. The general aim of the project was to improve the overall knowledge of the seismic hazard in order to reduce the earthquake risk in the area. In the framework of this project, this sector of the THV has been investigated.

Geophysical surveys (i.e., weak-motion recordings) of local and regional earthquakes, passive seismic noise, and gravity exploration have been collected in the THV. The buried shape of the valley was defined by separately inverting gravimetric data and horizontal-to-vertical spectral ratios (HVSRs) of ambient noise (Barnaba *et al.*, 2010).

Here, the seismic response of a sector of the THV is investigated from regional and local seismic events and ambient noise recordings. The uncertainty in the spectral response estimation is defined by taking into account results from classical standard spectral ratios (SSRs), generalized inversion techniques (GITs), and receiver functions (RFs) on subsets of data with different frequency bandwidths. The calculated local response is then convolved with the input motion from the 1976 M_w 6.4 Friuli mainshock recorded at the strong ground-motion site TLM1. Finally, the resulting pseudoacceleration response spectrum is compared with the elastic design spectrum of the current Italian regulation.

Geological and Geophysical Data

The THV is located in the northeastern corner of Italy, and it is part of the southern Alps. The floodplain of the river is a coverage of thick, loose coarse Quaternary sediments bounded by steep terraces of Permian–Triassic carbonate rocks and alluvial fans of loose and unconsolidated sediments. The tectonic framework appears to be very complex and mainly buried under the Quaternary coverage. The area is characterized by an east–west-trending system of south-verging thrusts and folds (see Fig. 1). Some backthrusts are still recognized. In general, the outcropping geology is fragmented into different tectonic wedges; the relationship between wedges and the deep tectonics is still unknown.

The area is one of the most active in the Alps; in the past it was shaken by medium- to strong-sized earthquakes that caused both heavy damage and many casualties. In particular, according to Bressan *et al.* (2003), the best documented historical events occurred in 1788 (I_0 = VIII–IX), 1908 (I_0 = VIII), 1928 (I_0 = IX), and 1959 (I_0 = VIII). Although the present level of seismicity is moderate, the permanent short-period seismic network of northeastern Italy (see Data and Resources) recorded three relevant events in this area: an M_L 5.2 earthquake on 16 September 1977, an M_L 4.2 earthquake on 1 February 1988, and an M_L 4.9 earthquake on 14 February 2002 (Ⓔ see Fig. S1 in the supplement). The area is close to the location of the 1976 M_w 6.4 Friuli earthquake (I_0 = IX).

The shape of the sediment-bedrock interface was constrained from gravimetric data and microtremors integrated by *S*-wave velocity profiles defined from surface-wave data. The subsurface structure of the valley was defined by interpreting the second-order polynomial residual gravity anomaly and the fundamental frequency of resonance estimated from the HVSR of ambient noise (Barnaba *et al.*, 2010; Ⓔ see Fig. S2 in the supplement). The maximum sediment thickness, in the southern part of the study area, is about 400 m, and a 150–200 m median value is recognized in the northern part (south of Tolmezzo; Ⓔ see Fig. S1 in the supplement). The valley width at the array is about 1600 m. The *S*-wave velocity profiles are characterized by lateral changes, as evidenced by the seismic surveys carried out within the valley (see Barnaba *et al.*, 2010). In the mid-valley, the *S*-wave velocity increases slowly with depth from about 600–800 m/s to 1200 m/s, to a shallow depth of 150 m. The profiles on the valley edge measure *S*-wave velocities lower than 400–600 m/s for a 40-m thick portion of shallow sediments. These *S*-wave velocities characterize the alluvial deposits: gravelly soils, cobbles, and coarse sediments are found in the mid-valley, though a higher proportion of sand and silt lenses characterize the valley edge near Cavazzo Carnico.

Earthquake Data

From 2004 to 2005 six stations were positioned along a profile across the THV in the Cavazzo Carnico plain

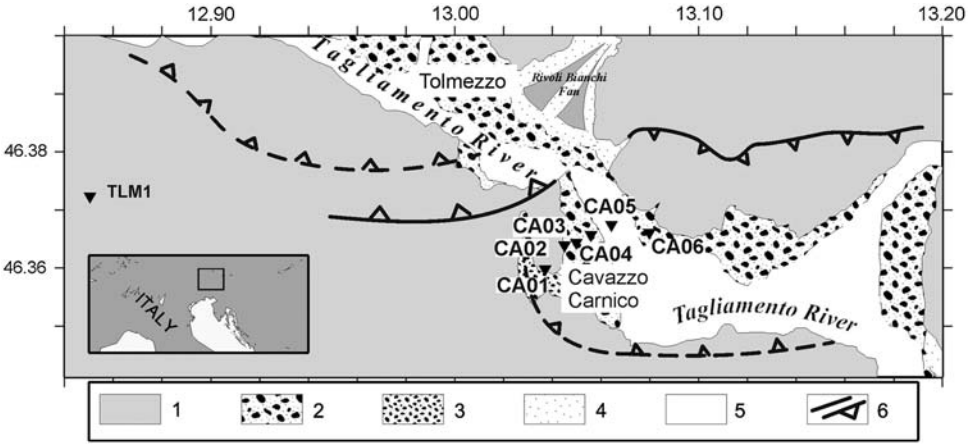

Figure 1. Geological sketch map of the Tagliamento high valley between Tolmezzo and Cavazzo Carnico (northeastern Italy). Main outcropping lithologies: 1, Permian–Triassic rocks; 2, coarse gravels; 3, sandy and silty soils; 4, alluvial fans; 5, present-day alluvium of the Tagliamento River and its tributaries; 6, main faults and thrusts. The seismic array within the valley is represented by stations CA01–CA06. TLM1 is the accelerometric station that recorded the 1976 M_w 6.4 Friuli earthquake.

(Fig. 1; Ⓔ see Table S1 in the supplement). Four stations (CA02, CA03, CA04, and CA05) were set within the valley at an interstation distance of about 200 m. Station CA06 was set on the eastern edge, just at the footwall of the main relief of the area, while CA01, the reference station, was set on the bedrock outcropping in the northern part of Cavazzo Carnico, outside the array.

Each station was equipped with an ORION Nanometrics data logger, a three-component sensor (Lennartz Le-3DLite) with a natural frequency of 1 Hz, a Global Positioning System (GPS) for time synchronization, and a power supply based on a solar panel system. Starting from June 2004, a continuous stream of data was stored over a period of 18 months, with a three-month switch off due to poor insulation during the winter (from December 2004 to March 2005). The dataset consisted of about 545 recorded earthquakes, but only 91 events with optimal signal-to-noise ratios (17% of the total; Ⓔ see Tables S2 and S3 in the supplement) are used in the following spectral analysis. The epicentral distances range from 10 to 400 km and the duration magnitude from M_D 1 to M_D 5.1. Waveforms from the 2004 Kobarid earthquake, located 40 km southeast of the array, are shown Ⓔ in Figure S3 in the supplement. Figure 2 shows the azimutal coverage in terms of the magnitude and distance of the earthquakes listed Ⓔ in Table S2 in the supplement.

Spectral Analysis on Earthquakes

Site responses are estimated considering the conventional SSR (Borcherdt, 1970), GIT (Andrews, 1986; Boatwright *et al.*, 1991), and RF techniques (Lermo and Chávez-García, 1994). For the different methods used here, our calculations assume the same input Fourier spectra. In the reference methods, the CA01 station represents the reference site. On local events (Ⓔ see Table S2 of the supplement), a 5.12-s fixed-length time window is selected, comprising the *S*-wave phase arrival. The time windows were automatically defined on each seismogram on the basis of a time-distance relation considering regional *S*-wave velocities. This allows the inclusion of the onset of the *S* waves within the analyzed windows. The horizontal components are taken into account by a vector sum using the complex time series technique of Steidl *et al.* (1996). The amplitude spectrum of complex time series provides the total amplitude of horizontal motion at a given frequency, thus preserving the phase between components.

Estimates of GIT at frequencies lower than 2 Hz are performed by using 20 s input data (Ⓔ see Table S3 in the supplement). The use of 23 regional earthquakes is advantageous to evaluate site factors at low frequencies because, far from the source, the source and path effects are considered to be common, and the vibrations cover a wide-frequency band.

The results shown in Figure 3 represent the mean values calculated from SSR, GIT, and RF methods. The two reference methods return similar results both for frequency and amplitude levels. Moreover, the GIT amplitude level is lower than SSR for CA06 site. This could be explained by the reduced number of events used in the SSR calculation for the CA06 site. Generalized inversion techniques have to be preferred to SSRs below 2 Hz because of the 20-s input data used.

The shape and level of the amplification curves between the different site response methods agree well in the frequency range from 1 to 10 Hz. However, variable levels of amplification are observed in the RF method, where, in comparison with GIT and SSR, we find a lower response. The response underestimation by RF was observed elsewhere by other authors (e.g., Field and Jacob, 1995; Parolai *et al.*, 2000) and often explained by focusing/defocusing effects. GITs and RF responses differ mainly at the CA02 and CA03 sites that are influenced by the valley edge.

Considering all the reference and nonreference methods, the CA02 site shows the highest response, while site CA05 (in the middle of the valley) is characterized by the lowest one. Shallow *S*-wave velocities at the mid-valley are faster than those at the valley edge; this could partially explain the different response (Barnaba *et al.*, 2010).

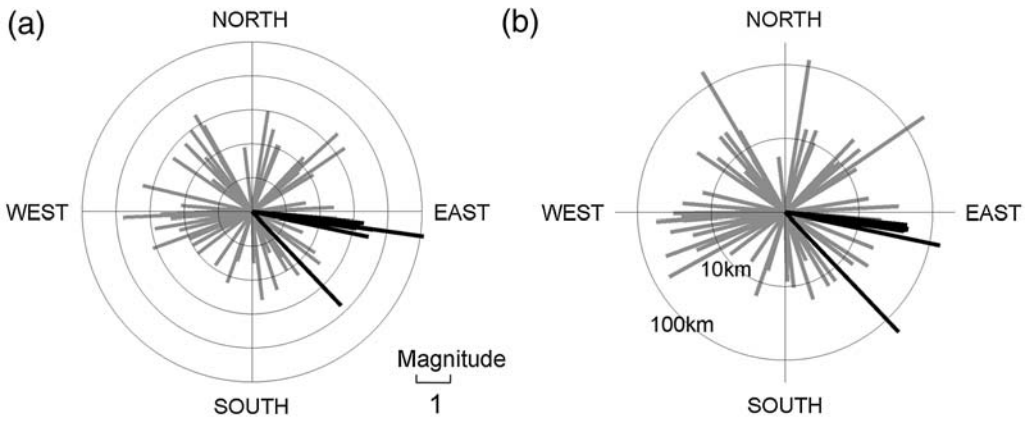

Figure 2. Polar diagrams of the azimuthal coverage as a function of (a) magnitude and (b) distance provided by the 67 earthquakes listed Ⓔ in Table S2 in the supplement. Thick black lines highlight the events of the Kobarid seismic sequence (close to 95°) and two other events far from the array (Ⓔ see events listed in bold in Table S2 in the supplement).

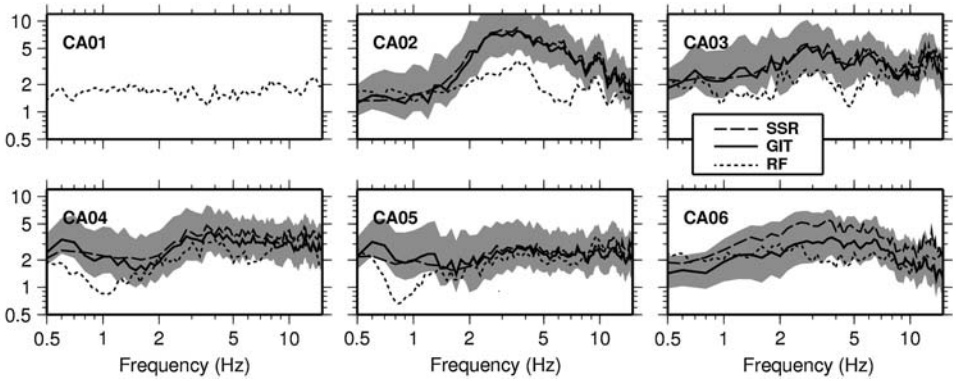

Figure 3. Mean spectral ratio estimates of site response using SSRs (dashed line), GITs (bold line), and RFs (dotted line). CA01 represents the reference site for GITs and SSRs. The shadowed light gray areas define the standard deviation bounds for GIT calculations.

GITs and SSRs show clear peaks of amplifications at mid-valley sites CA04 and CA05 at low frequencies (0.55–0.6 Hz) around the fundamental frequency of resonance of the valley (see numerical simulations described in Barnaba *et al.*, 2010).

In considering RF responses, we can observe that the amplification at 0.55–0.6 Hz is present all along the linear array, and even at the reference site CA01. To investigate the reason for the low-frequency amplification at the reference site CA01, we evaluate the RF response, sorting the input data into two different subsets: (1) randomly selected local earthquakes and (2) events from the south-southeast quadrant, mainly located in the Kobarid area (see Fig. 2 and events in bold Ⓔ in Table S2 in the supplement). The longitudinal axis of the valley in the southern part is aligned with the Cavazzo–Kobarid path (Ⓔ see Fig. S1 in the supplement). The RF response of the events coming from a random azimuth (Fig. 4a) can be compared with RF data obtained from the Kobarid area events (Fig. 4b) at the CA01 site. While we can observe a random pattern of spectral amplitudes in Figure 4a, with an almost flat response, a clear amplification peak is evidenced in Figure 4b at 0.55–0.6 Hz.

The low-frequency peak can be observed even at sites within the valley but generally with an increased amplitude level. Earthquake magnitudes in the Kobarid seismic data range from M_L 2.8 to M 5.1, and the amplification in the low-frequency band is independent of the earthquake size. These observations suggest that the seismic waves from the Kobarid sequence, excited at 40–45 km distance from the array, travel along a 6-km-long valley segment, with longitudinal axis aligned with the Kobarid–Cavazzo Carnico azimuthal path. The spectral amplitude enhancement is probably due to guided waves channeled within the sediment fill that give rise to a weak 2D to 3D response because of the deepening of the valley toward the south (Ⓔ see Fig. S2 in the supplement).

Noise Analysis

The seismic array close to Cavazzo Carnico, which operated in continuous mode for 18 months, allowed the recording of a large amount of data. The single station HVSR and reference-site noise analysis are performed. Thirty-minute time windows of randomly selected ambient noise, from day to night both in the summer and winter, are analyzed. A selection of the time windows was performed in order to retain the most stationary parts of the noise, avoiding the anomalous spikes or transients often associated with specific sources (e.g., walking, traffic). The spectral analysis is performed on multiple cosine-tapered 180-s-long windows of the signal. Horizontal-to-vertical spectral ratio curves are generally consistent with the spectral ratios from recorded earthquakes (see Fig. 5).

Mid-valley CA04 and CA05 sites are characterized by a low-frequency fundamental resonance below 1 Hz (see Fig. 5) and by secondary peaks at higher frequencies. Higher frequencies are amplified at the valley edges (3–5 Hz and

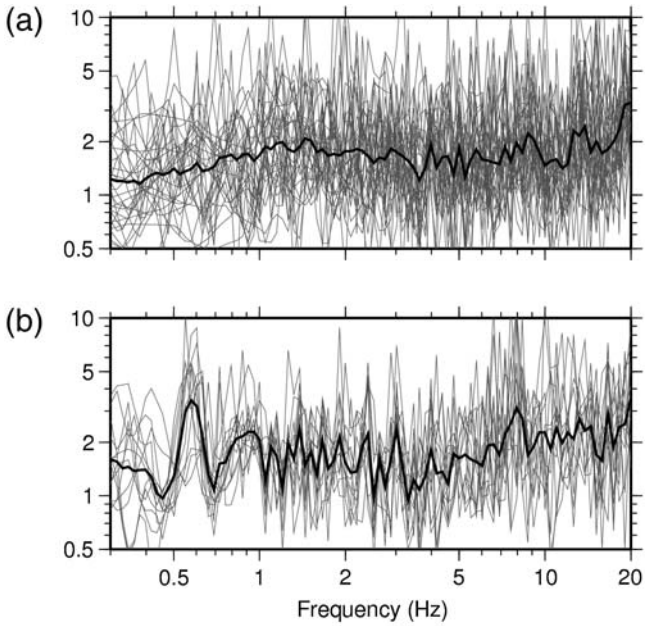

Figure 4. CA01 site RF spectral response: (a) RF defined for randomly sorted events; (b) RF defined for Kobarid seismic sequence events. The bold line represents the resulting mean value while gray curves represent the RF spectral ratios from a single earthquake.

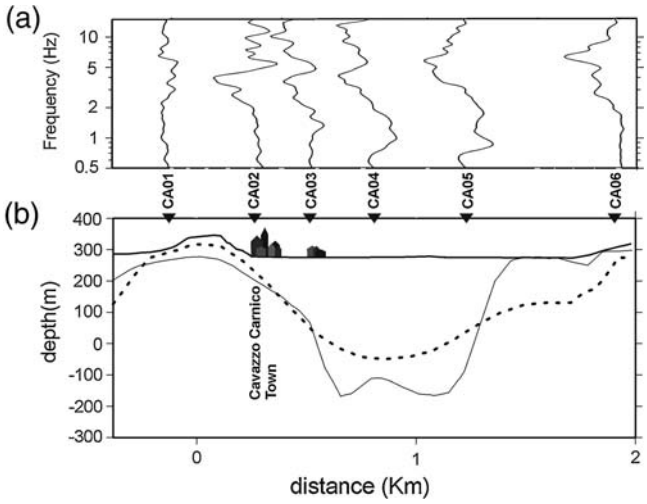

Figure 5. (a) HVSR estimated at the array of stations along the THV profile. Thirty-minute time windows of ambient noise are used. (b) The dashed line shows the buried morphology obtained by gravity; the solid line shows the microtremor analysis in Barnaba *et al.* (2010).

6–7 Hz at CA02 and CA06, respectively). Horizontal-to-vertical spectral ratios are in agreement with *S*-wave velocity profiles shown in Barnaba *et al.* (2010) (Ⓔ see Fig. S4 in the supplement) and feature spectral amplitudes that are comparable with SSR and GIT.

Reference-site noise analysis is applied rotating the horizontal components to the longitudinal (N150°E, corresponding to the valley elongation) and to the transverse (N60°E) axis of the valley, respectively. As shown in Barnaba *et al.* (2010) in this specific case and by many other authors (e.g., Steimen *et al.*, 2003; Roten *et al.*, 2006), this latter method is preferable to detect the frequency of resonance, because peaks often appear sharper than those found on HVSRs. Figure 6 confirms the results obtained by Barnaba *et al.* (2010), whereby the fundamental frequency of resonance at mid-valley sites was found to be below 1 Hz for both the radial (*SV*) and transverse (*SH*) components.

Site-Specific Pseudoacceleration Response Spectra

During the 1976 Friuli earthquake the accelerometric station TLM1 located 3 km west of the Cavazzo Carnico array recorded the mainshock with a peak acceleration value of about 350 cm/s^2. The distance from TLM1 to the epicentral area is about 20 to 25 km. In Barnaba *et al.* (2007), the TLM1 site response is analyzed to evaluate a possible influence of the dam-reservoir system and surrounding hills close to the strong-motion site. By filtering the specific site response measured at the TLM1 station, Barnaba *et al.* (2007) obtained a reduction of the peak acceleration to about 188 cm/s^2. Site-correction factors for TLM1 with respect to a rock site determined by Barnaba *et al.* (2007) are applied here and used as input motion for evaluating the Cavazzo Carnico local response during the 1976 mainshock. This could be of some interest because it allows the pseudoacceleration response spectra to be compared with the elastic demand of the current regulations. Moreover, it could help in explaining the heavy damage in Cavazzo Carnico caused by the 1976 Friuli earthquake.

Thus, horizontal components of accelerometric data are convolved here with the mean GIT response shown in Figure 3. The 5%-damped pseudoacceleration response spectra are subsequently obtained by averaging CA02 and CA03 sites to obtain a local response representative of the valley edge. At the same time, CA04 and CA05 are averaged for estimating the mid-valley response spectra. Figure 7 shows the comparison of the elastic demand spectra of the current national regulations specific for Cavazzo Carnico (return period of 475 years and ordinary buildings) and the 5%-damped pseudoacceleration response spectra.

The results of Figure 7a suggest that the current regulations (life safety spectra) are not adequate for Cavazzo

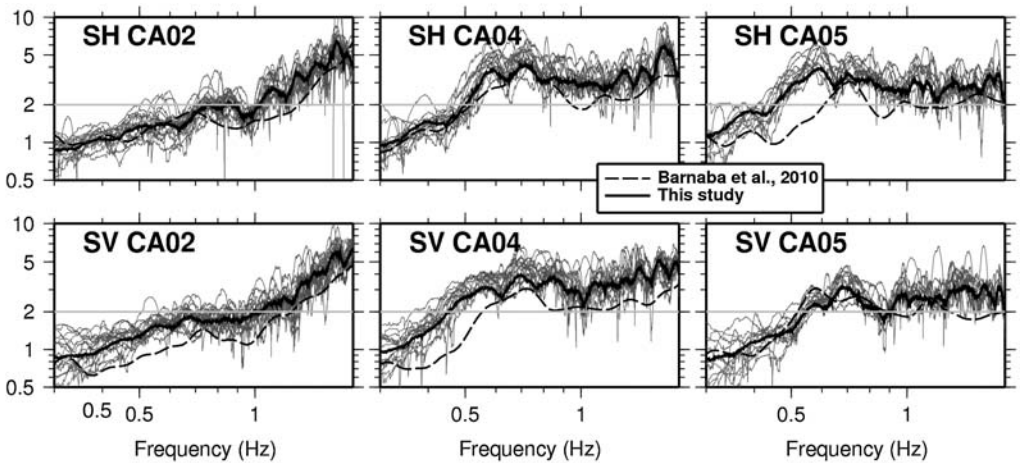

Figure 6. (top) *SH* and (bottom) *SV* horizontal spectral ratios of ambient noise with respect to CA01 site. Thirty-minute time windows of ambient noise are used. Each time window is represented by a thin gray line, while the bold black line is the resulting mean value (CA02, left panels; CA04, central panels; and CA05, right panels).

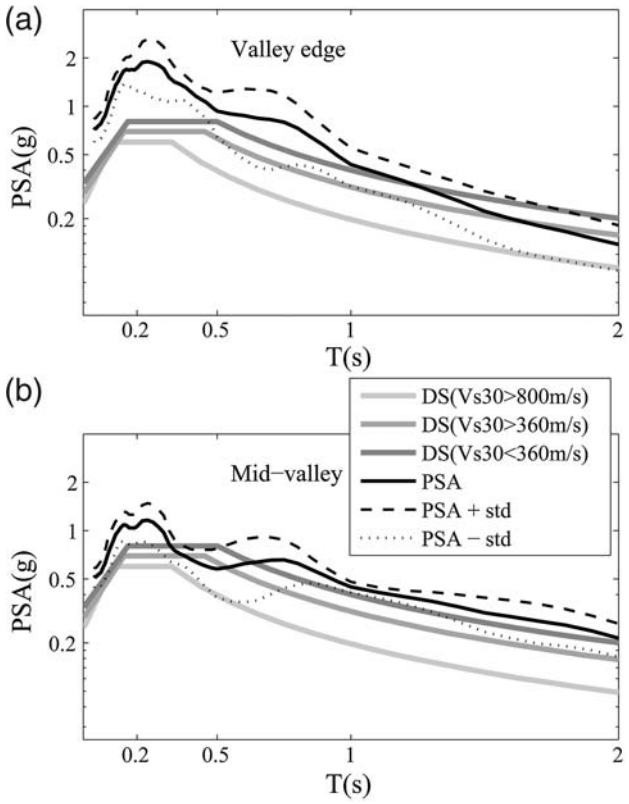

Figure 7. Five-percent-damped pseudoacceleration response spectra estimations (solid black line) compared with elastic demand spectra of the current Italian regulations (solid gray lines). Demand spectra are provided for A (V_{S30} > 800 m/s), B (V_{S30} > 360 m/s), and C (V_{S30} < 360 m/s) type sites, return period of 475 years, and ordinary buildings. Pseudoacceleration spectra are averaged from the two horizontal components of ground motion and stations at (a) the valley edge and (b) at mid-valley.

Carnico, where large local effects due to the valley edge could be expected. Calculated pseudoacceleration spectra overcome the current regulations demand in the frequency range from 2 to 10 Hz at the CA02–CA03 sites. On the other hand, the pseudoaccelerations estimated at the CA04–CA05 sites at the mid-valley agree well with the elastic demand spectra provided by national regulations.

Gallipoli and Mucciarelli (2009) found that for one-third of examined sites in Italy, V_{S30} does not represent a good proxy of observed amplification. They used mainly earthquake RFs to estimate the response at sites characterized by simple 1D velocity layering. We compare our results in Cavazzo Carnico with average RFs obtained by Gallipoli and Mucciarelli (2009) in Figure S5 Ⓔ in the supplement. Estimates for V_{S30} at the valley edge and at mid-valley are about 410 m/s and 540 m/s, respectively (Ⓔ see Fig. S4 in the supplement). Generalized inversion techniques estimated at the valley edge returns amplification considerably higher than the averaged RFs from Gallipoli and Mucciarelli for both B and C sites.

Generalized inversion techniques and RF amplifications in Cavazzo Carnico are then normalized by calculating an adimensional parameter similarly to that of Gallipoli and Mucciarelli. Negative values of the adimensional parameter ε (see Gallipoli and Mucciarelli, 2009 for details and Ⓔ Fig. S6 in the supplement) define ranges of seismic code underestimation of observed amplification. Code underestimation by RF at the valley edge is consistent with Gallipoli and Mucciarelli (site B) up to 6.5 Hz. Considering GIT, the underestimation becomes larger than RF and that described by Gallipoli and Mucciarelli (more than one standard deviation from 2.3 Hz up to 10 Hz for class B). The most plausible explanation to account for these observations is constructive interference between edge-generated surface waves and the delayed direct arrival, commonly referred to as the basin-edge effect.

Discussion and Conclusions

We have analyzed the seismic response of the THV at the Cavazzo Carnico plain due to earthquakes and ambient noise. During the 18 months of continuous recordings, a large quantity of data was collected, including the mainshock of the Kobarid sequence (M_L 5.1). Standard spectral ratios and GIT reference methods show consistent results. Slight differences arise in the two different subsets of data used. However, 90% of the events used have been recorded at all six stations. A lower level of amplification by the RF method in comparison with GITs and SSRs is generally observed. All the methods show higher amplification in the frequency range from 2 to 8 Hz and mostly at the valley edges. The sites in the middle of the valley enhance lower frequencies (0.55–0.6 Hz) that represent the fundamental frequency of resonance of the valley. The amplification in this frequency range can also be observed in the RF method, but with variable spectral amplitudes at different sites. The Kobarid seismic sequence is able to excite a low-frequency band (0.55–0.6 Hz) at all the sites. The spectral amplitude enhancement observed at 0.55–0.6 Hz, even recorded at the reference site CA01, is interpreted here as a channeling effect of guided waves within a deep 6-km-long valley sediment fill. Results from ambient noise analysis agree well with the site responses estimated from earthquake based methods.

Finally, the elastic demand spectra of the current national regulations for Cavazzo Carnico are compared with the site-specific 5%-damped pseudoacceleration response spectra. The comparison suggests that the current regulations underestimate the large amplification effect due to the valley edge in Cavazzo Carnico.

Data and Resources

Events recorded by the temporary array of seismic stations were localized by the short-period seismometric network of northeastern Italy, run by the Istituto Nazionale di Oceanografia e di Geofisica Sperimentale (OGS). Locations of the historical events were found in DOM 4.1 at http://emidius.mi.ingv.it/DOM (last accessed November 2011), while parameters for instrumental events were

retrieved from the OGS Bulletin at http://www.crs.inogs.it/bollettino/RSFVG (last accessed August 2012). Regional earthquakes were located by using the catalog from the European-Mediterranean Seismological Centre. MCS intensities are retrived from the Italian macroseismic catalog DBMI04 at http://emidius.mi.ingv.it/DBMI04 (last accessed August 2012). The demand spectra, as specified by the Italian code for target performance levels of life safety ($T_r = 475$ years) and for B and C sites, were obtained using the software provided by Consiglio Superiore dei Lavori Pubblici (Spettri-NTC v. 1.03) at http://www.cslp.it (last accessed August 2012). Detailed information about the SISMOVALP project can be found at http://www-lgit.obs.ujf-grenoble.fr/sismovalp (last accessed April 2010).

Acknowledgments

We are grateful to the technical staff of the OGS Centro di Ricerche Sismologiche (CRS) for their efforts in the maintenance of the stations. This research was funded by the European Union under the INTERREG IIIB-Alpine Space framework, project number F/I- 2/3.325 entitled "SISMOVALP—Seismic Hazard and Alpine Valley Response Analysis", and the Italian Ministry of the University and Research (MIUR). We would like to acknowledge Enrico Priolo, Marco Mucciarelli, and Arben Pitarka for their useful comments and suggestions.

References

Andrews, D. J. (1986). Objective determination of source parameters and similarity of earthquakes of different size, in *Earthquake Source Mechanics*, S. Das, J. Boatwright, and C. H. Scholz (Editors), Geophys. Monograph Series, American Geophysical Union **37,** 259–268.

Bard, P. Y., and M. Bouchon (1985). The two-dimensional resonance of sediment-filled valleys, part II: The case of incident *P* and *SV* waves, *Bull. Seismol. Soc. Am.* **75,** 519–541.

Barnaba, C., L. Marello, A. Vuan, F. Palmieri, M. Romanelli, E. Priolo, and C. Braitenberg (2010). The buried shape of an Alpine valley from gravity surveys, seismic and ambient noise analysis, *Geophys. J. Int.* **180,** no. 2, 715–733.

Barnaba, C., E. Priolo, A. Vuan, and M. Romanelli (2007). Site effect of the strong-motion site at Tolmezzo-Ambiesta Dam in northeastern Italy, *Bull. Seismol. Soc. Am.* **97,** no. 1B, 339–346.

Boatwright, J., J. B. Fletcher, and T. E. Fumal (1991). A general inversion scheme for source, site, and propagation characteristics using multiply recorded sets of moderate-sized earthquakes, *Bull. Seismol. Soc. Am.* **81,** 1754–1782.

Borcherdt, R. D. (1970). Effects of local geology on ground motion near San Francisco Bay, *Bull. Seismol. Soc. Am.* **60,** 29–61.

Bressan, G., P. L. Bragato, and C. Venturini (2003). Stress and strain tensors based on focal mechanisms in the seismotectonic framework of the Friuli-Venezia Giulia region (northeastern Italy), *Bull. Seismol. Soc. Am.* **93,** no. 3, 1280–1297.

Brisighella, L., L. Cappellari, B. Dall'Aglio, R. D'Eredità, R. Gori, L. Simoni, G. Turrini, and F. Zaupa (1976). Earthquake in Friuli (Italy)-1976. Damage to historical monuments and other buildings of artistic interest, *Boll. Geof. Teor. Appl.* **19,** 1203–1452 (in Italian).

Chávez-García, F. J., J. Castillo, and W. R. Stephenson (2002). 3D site effects: A thorough analysis of a high-quality dataset, *Bull. Seismol. Soc. Am.* **92,** no. 5, 1941–1951.

Fäh, D., P. Suhadolc, and G. F. Panza (1993). Variability of seismic ground motion in complex media: The case of a sedimentary basin in the Friuli (Italy) area, *J. Appl. Geophys.* **30,** 131–148.

Field, E. H. (1996). Spectral amplification in a sediment-filled valley exhibiting clear basin-edge-induced waves, *Bull. Seismol. Soc. Am.* **86,** no. 4, 991–1005.

Field, E. H., and K. H. Jacob (1995). A comparison and test of various site-response estimation techniques, including three that are not reference-site dependent, *Bull. Seismol. Soc. Am.* **85,** 1127–1143.

Frischknecht, C., and J.-J. Wagner (2004). Seismic soil effect in an embanked deep Alpine valley: A numerical investigation of two-dimensional resonance, *Bull. Seismol. Soc. Am.* **94,** no. 1, 171–186.

Gallipoli, M. R., and M. Mucciarelli (2009). Comparison of site classification from V_{S30}, V_{S10}, and HVSR in Italy, *Bull. Seismol. Soc. of Am.* **99,** no. 1, 340–351.

Kagami, H., C. M. Duke, G. C. Liang, and Y. Ohta (1982). Observations of 1- to 5-second microtremors and their application to earthquake engineering. Part II: Evaluation of site effect upon seismic wave amplification due to extremely deep soil deposits, *Bull. Seismol. Soc. Am.* **72,** 987–998.

Kawase, H. (1996). The cause of the damage belt in Kobe: "The basin-edge-effect", constructive interference of the direct *S* wave with the basin-induced diffracted/Rayleigh waves, *Seismol. Res. Lett.* **67,** no. 5, 25–34.

Lermo, J., and F. J. Chávez-García (1994). Are microtremors useful in site response evaluation? *Bull. Seismol. Soc. Am.* **84,** no. 5, 1350–1364.

Parolai, S., D. Bindi, and P. Augliera (2000). Application of the generalized inversion technique (GIT) to a microzonation study: Numerical simulations and comparison with different site-estimation techniques, *Bull. Seismol. Soc. Am.* **90,** 286–297.

Pedersen, H. A., M. Campillo, and F. J. Sánchez-Sesma (1995). Azimuth dependent wave amplification in alluvial valleys, *Soil Dynam. Earthquake Eng.* **14,** 289–300.

Roten, D., D. Fäh, C. Cornou, and D. Giardini (2006). Two-dimensional resonances in Alpine valleys identified from ambient vibration wavefields, *Geophys. J. Int.* **165,** 889–905.

Steidl, J. H., A. G. Tumarkin, and R. Archuleta (1996). What is a reference site? *Bull. Seismol. Soc. Am.* **86,** 1733–1748.

Steimen, S., D. Fäh, F. Kind, C. Schmid, and D. Giardini (2003). Identifying 2D resonance in microtremor wave fields, *Bull. Seismol. Soc. Am.* **93,** 583–599.

Stucchi, M., R. Camassi, A. Rovida, M. Locati, E. Ercolani, C. Meletti, P. Migliavacca, F. Bernardini, and R. Azzaro (2007). DBMI04, il database delle osservazioni macrosismiche dei terremoti italiani utilizzate per la compilazione del catalogo parametrico CPTI04, *Quaderni Geofisc.* **49,** 38 (in Italian; available at http://emidius.mi.ingv.it/DBMI04/, last accessed August 2012).

Tucker, B., and J. King (1984). Dependence of sediment-filled valley response on input amplitude and valley properties, *Bull. Seismol. Soc. Am.* **74,** 153–166.

Centro di Ricerche Sismologiche
Istituto Nazionale di Oceanografia e di Geofisica Sperimentale (OGS)
Via Treviso, 55
33100 Cussignacco (Udine)
Italy
cbarnaba@inogs.it
(C.B.)

Centro di Ricerche Sismologiche
Istituto Nazionale di Oceanografia e di Geofisica Sperimentale (OGS)
Borgo Grotta Gigante 42/C
34010 Sgonico (Trieste)
Italy
avuan@inogs.it
(A.V.)

Manuscript received 13 March 2012